Discreteness effects in cosmological N-body simulations

James Binney

Theoretical Physics, 1 Keble Road, Oxford OX1 3NP

ABSTRACT

An estimate of the convergence radius of a simulated CDM halo is obtained under the assumption that the peak phase-space density in the system is set by discreteness effects that operate prior to relaxation. The predicted convergence radii are approximately a factor 2 larger than those estimated for numerical convergence studies.

A toy model is used to study the formation of sheets of the cosmic web, from which DM haloes form later. This model demonstrates the interplay between phase mixing and violent relaxation that must also be characteristic of spherical collapse. In the limit that sheets contain arbitrarily many particles, it seems that power-law profiles are established in both distance and energy. When only a finite number of particles is employed, relaxation is prematurely terminated and the power laws are broken. In a given simulation, the sheets with the highest peak phase-space densities are those that form from the longest waves. Hence simulations with little small-scale power are expected to form the cuspiest haloes.

Key words: methods: *N*-body simulations – galaxies: formation – cosmology: dark matter.

1 INTRODUCTION

Cold Dark Matter (CDM) is thought to dominate structure formation through gravitational clustering. As its name implies, this material starts out very cold, so that to an excellent approximation particles are confined to a three-dimensional surface $[\mathbf{r}, \mathbf{p(r)}]$ in six-dimensional phase space. The distribution function f is infinite on this surface and zero elsewhere. The fine-grained distribution function is constant because it obeys the collisionless Boltzmann equation. Hence, very high phase-space densities are in principle possible right up to the present epoch.

Studies of structure formation rely heavily on *N*-body simulations to follow the clustering of dark matter (DM). Galaxies are believed to form from baryons that have fallen in to the centres of DM haloes, so the implications of various theories of DM for the observable properties of galaxies depend sensitively on the small-scale structure of dark haloes. Hence, it is important to understand how accurately *N*-body simulations represent the inner parts of dark haloes, and this problem has attracted considerable attention (Jing et al. 1995; Klypin et al. 2001; Taylor & Navarro 2001; Navarro 2003; Power et al. 2003; Fukushige, Kawai & Makino 2003; Hayashi et al. 2003).

On sufficiently small scales it is clear that the simulations will become untrustworthy because they employ only a finite number of particles (Kuhlman et al., 1996; Melott et al., 1997; Splinter et al., 1998; Binney & Knebe, 2002).

Generally this scale is determined by resimulating a given halo with improved resolution, in terms of the number of particles employed, the number of waves used to define the initial conditions, the smallness of the gravitational softening parameter ϵ, and the smallness of the timesteps. Based on such simulation series, Power et al. (2003) define a radius $r_{\rm conv}$ outside which a given simulated halo should be reliable, by calculating the smallest radius at which three criteria are all met: (i) the local orbital time is much longer than the numerical timestep; (ii) the centripetal acceleration of a circular orbit is smaller than $0.5V_{200}^2/\epsilon$, where V_{200} is the halo's characteristic velocity; and (iii) the local two-body relaxation time is longer than the Hubble time.

While it is clear that satisfaction of all three criteria is a necessary conditions for a N-body simulation to be credible, it is not clear that it is a sufficient condition: errors in the integration of the equations of motion at any cosmic epoch can invalidate the final halo. We argue here that a particularly important epoch to get right is the one that ends when overdensities first collapse to form sheets that are virialized in only one direction. We present evidence that discreteness effects at this primary stage, rather than, for example, two-body relaxation in virialized haloes, are what limit the central densities of simulated haloes.

We use a toy model and analytic calculations to clarify what happens when virialized CDM structures form, and to understand the extent to which N-body simulations of structure formation are compromised by artifacts due to discrete-

ness. The model explains why cuspy profiles form even when power at high spatial frequencies is removed from the initial fluctuation spectrum. It also suggests that in the absence of discreteness effects, virialized haloes would have power-law cusps. Finally analytic arguments are used to estimate the radius in a simulated halo within which the central profile is flattened by discreteness effects that operate prior to virialization, and we show that these estimates are in good agreement with the latest numerical convergence studies.

2   A TOY MODEL

In this section we use a one-dimensional toy system to study the interplay between phase mixing and violent relaxation, and to show how discreteness cuts short this interplay. The simulations of Melott (1983) are similar, except that they are for hot dark matter and they employ a conventional particle-mesh N-body technique to advance the particles.

Consider the dynamics of an odd number $2n+1$ of flat mass sheets that are all perpendicular to the x axis and move parallel to this axis. To avoid confusion later, we henceforth call these sheets 'particles'. The particles, which each have surface density Σ/n, interact only through gravity. There is no net force on the middle particle. Let k be the rank of a particle with respect to this middle particle, with $k < 0$ for particles on its left. Then the particle with rank k experiences a force $F_k = -4\pi G\Sigma(k/n)$ that only changes when the particle passes through another particle. Hence the particle's location, $x_k(t)$, is quadratic in time between such passages. So we can analytically solve for the instant at which the next passage occurs, and update the phase-space coordinates of the particles to this time to machine precision. The ranks of the passing particles are then exchanged and we solve for the instant of the next passage. Hence this model provides a convenient laboratory for a high-precision study of virialization.

We adopt initial conditions appropriate to the moment of turnaround of an overdense region of the Universe. The ranking of the particles will not have changed up to this time, so the requirement that at some fixed time τ in the past, all particles were located at the origin becomes

$$x_k - v_k\tau - 2\pi G\Sigma(k/n)\tau^2 = 0 \qquad (k = -n, \ldots, n). \qquad (1)$$

This set of equations has a solution that corresponds to a homogeneous distribution at turnaround

$$x_k = 2\pi G\Sigma\tau^2(k/n), \quad v_k = 0. \qquad (2)$$

If we define $X_k = x_k - x_{k-1} - 2\pi G\Sigma\tau^2/n$ and $V_k = v_k - v_{k-1}$, then equations (1) yield a relation between X_k and V_k, namely

$$V_k = \frac{X_k}{\tau}. \qquad (3)$$

Fig.1 shows from top left to bottom right six stages in the relaxation of 301 particles from the initial conditions obtained by choosing

$$X_k = -0.6\frac{\pi G\Sigma\tau^2}{n}\cos(0.3\pi k/n). \qquad (4)$$

The time, in units of τ, since these initial conditions were imposed is given in the top left corner of each panel. The negative slope in the top left panel implies that at the start of
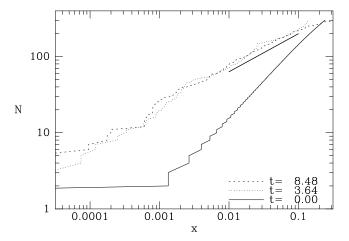

Figure 2. The number of particles with $|x|$ less than a given value at three times. The bold line shows the slope for $N \propto |x|^{1/2}$.

the simulation, the system is already collapsing. In the next panel ($t = 0.4$) the vertical orientation of the distribution near the origin indicates that the centre has at that time finished collapsing. By the time, $t = 1.64$, of the next panel, the centre has expanded and collapsed once more. The edge, by contrast, is still in full collapse. The following panels show that the phase lag ψ between the oscillations of the centre and the outside grows rapidly. By the time, $t = 9.7$, of the last panel, ψ is many π, and near the centre it has become hard to follow the spiral of phase points.

Fig. 2 explores the evolution of the density profile of this system by plotting the cumulative number of particles with $|x|$ less than any given number at three times. In this logarithmic plot, the curve for $t = 0$ has unit slope to within the errors because the density of particles $\rho \sim$ constant initially. The slopes of the other two curves are near $\frac{1}{2}$, which implies $\rho \sim x^{-1/2}$.

By Jeans' theorem, the distribution function of the equilibriated system must be a function $f(E)$ of energy $E = \frac{1}{2}v^2 + \Phi$. From the fact that the force law is

$$F(x) = -4\pi G\Sigma(x/x_{\max})^{1/2}, \qquad (5)$$

where $x_{\max}$ is of order the amplitude of oscillation of the least bound particles, it is easy to show that the power-law nature of the density profile implies that

$$f = f_0 E^{-5/6}, \qquad (6)$$

where

$$f_0 = 2^{-3/2}\left(\frac{\pi G\Sigma^4}{3x_{\max}^2}\right)^{1/3}\bigg/\int_0^\infty \frac{\mathrm{d}y}{(y^2+1)^{5/6}}\;. \qquad (7)$$

Two processes are manifest in Fig. 1. (i) The winding up of the line of phase points into an ever tighter spiral is phase mixing. (ii) Violent relaxation in the sense of Lynden-Bell (1967) causes the edge of the occupied part of the phase plane to move outwards, and the points near the centre to move towards the origin: the system's time-varying gravitational field is transferring energy from the central to the peripheral particles. The process by which this energy transfer occurs is this. Between the top left and top right panels, the particles that are at $|p_x| \lesssim 0.2$ in the second figure have fallen together under their mutual self gravity. Particles fur-
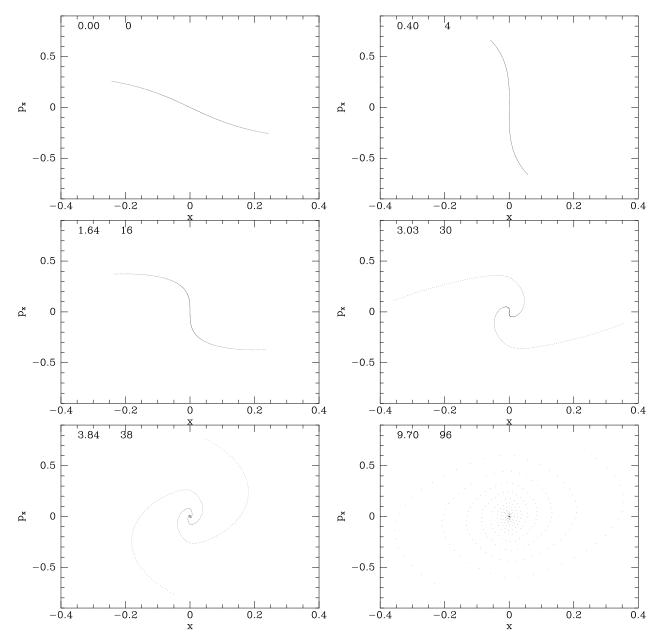
Figure 1. From top left to bottom right, six stages in the violent relaxation of 301 particles. The number in the top left corner of each panel is the time since the initial conditions of equations (4) were imposed. The units of time are the turnaround time τ of the underlying homogeneous distribution of particles.

ther out have not been affected by this infall. However, when the inner particles expand, the outer particles are falling in past them, and the inner particles have to climb out of a deeper well than they fell into. Conversely, the outer particles fall into a well that has significantly weakened by the time they rise up the other side.

This transfer of energy from the inner to the outer particles increases the density contrast between the centre and the outside. Since the frequency of a particle's oscillations through the centre scales as the square root of the mean density $\overline{\rho}$ interior to it, the energy transfer enhances the rate at which the function $\psi(E)$ is steepening. The energy transfer works most effectively between groups of particles that differ by $\sim \pi/4$ in ψ. So, as the first five panels of Fig. 1 clearly

show, the characteristic distance scale of the transfer rapidly decreases. In a useful, if oversimplified[1] picture, the first collapse transfers energy between the inner and the outer half of the particles. The second collapse at the centre transfers energy from the first quartile to the second quartile, and a little later energy is transferred from the second to the third quartile, and later still on out to the fourth quartile. By this time the additional central collapse pictured in the fourth panel of Fig. 1 is transferring energy from the innermost $\frac{1}{8}$ of the particles, and so on. At each stage the transfers become smaller because they involve a smaller and smaller fraction

---

[1] The actual numbers of particles (out of 301) losing energy at successive central collapses are $\sim$ 100, 44, 28 and 19.
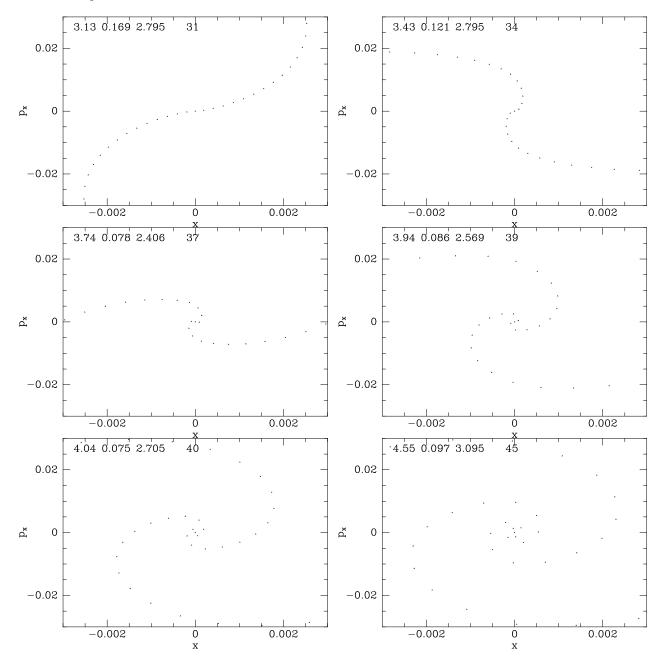
Figure 4. As Fig. 1 but zoomed in on the centre of phase space and at comparatively late times.

of the mass, but Fig. 3 shows that they remain significant to remarkably late times.

Fig. 4 shows zoomed-in views of the centre of phase space at six fairly late times. In the first three panels the spiral of phase points is unmistakable, but in the last three panels it has become hard to trace because it bends through a large angle between points. In these circumstances violent relaxation can no longer transfer energy between particles, and the increase in the central mass density ceases. Fig. 3 confirms this conclusion by showing that the energy of the innermost particles stops decreasing at about the time, $t = 4.04$, of the bottom left panel of Fig. 4.

The last panel of Fig. 4 gives the impression that the system has a finite central phase-space density. If we re-ran the simulation with more particles, we would be able to trace

the spiral even at this time, and the impression of a finite central phase-space density would be dispelled. Violent relaxation would continue to later times and generate a higher central mass density. Fig. 3 shows that once the phase-space spiral has ceased to be resolved, the energy of the innermost particles increases, presumably as a manifestation of two-body relaxation (i.e., stochastic heating).

In is interesting to quantify the peak phase space density. This will be of order Γ^{-1}, where Γ is the Poincaré invariant of the orbit of particles with rank $|k| \sim 2$. From the force law (5) the energy equation is

$$\tfrac{1}{2}\dot{x}^2 = 4\pi G\Sigma \frac{2}{3\sqrt{x_{\max}}} \left(X^{3/2} - x^{3/2} \right), \tag{8}$$

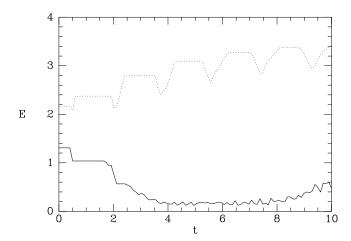where X is the amplitude of a particle's oscillations. Equat-

Figure 3. Energy of the innermost 8 particles (full curve) and outermost 8 particles (dotted curve) as a function of time. For clarity the energy of the inner particles has been multiplied by 2000.

ing Γ to the product of X and the corresponding peak speed for orbits with $|k| = 2$, we find

$$f_{\max} \sim \frac{1}{\Gamma} = \left(\tfrac{16}{3}\pi G\Sigma x_{\max}^3\right)^{-1/2} \left(\frac{n}{2}\right)^{7/2}. \qquad (9)$$

This equation can be exploited in two ways. First we can consider the effect of increasing the numerical resolution at which a given structure is simulated. Then n increases while the other factors are constant, so the peak value of the DF rises steeply with n.

Alternatively, we can apply equation (9) to a series of structures within a given simulation. Then Σ and $x_{\max}$ are both proportional to n, so overall $f_{\max} \sim n^{3/2}$. Hence the highest phase-space densities are to be found in the largest structures, because it is in these structures that violent relaxation works most efficiently.

2.1 Case of finite initial phase-space density

Consider the case in which the initially populated region of phase space has a finite width – as in the case of warm dark matter. The winding up of the spiral and violent relaxation will proceed as before until the spiral's radius of curvature becomes comparable with the width of the populated sheet. At this point violent relaxation ceases to be possible. Hence, the peak phase-space density of the relaxed system will be comparable to the initial phase-space density of the sheet. Melott (1983) reached a similar conclusion on the basis of his simulations of pancake formation in a hot-dark-matter cosmology.

2.2 Summary of experimental results

From our one-dimensional example we conclude the following

(i) Material at each distance from the centre executes os-cillations. The phase of these oscillations becomes a progres-sively steeper function $\psi(E)$ of distance from the centre of phase space.

(ii) Gravity transfers energy with great efficiency between particles whose oscillations are out of phase by $\sim \pi/4$. Even a small initial enhancement of density towards the centre causes this transfer to be outward.

(iii) The outward transfer of energy enhances the density contrast, which steepens the function $\psi(E)$, and reduces the length scale over which individual energy transfers occur.

(iv) Outward energy transfer continues until the underly-ing spiral in phase space ceases to be resolved in the sense that the spiral turns through a large angle between phase points.

(v) In the limit of an arbitrarily large number of particles, the spiral remains resolved through arbitrarily many wind-ings, and the density profile of the final relaxed structure is strictly singular.

(vi) The large dynamic range between the smallest lengthscale of energy transfer and the overall system size, combined with the hierarchical nature of the energy trans-fer process serve to establish a power-law density profile $\rho \sim x^{-1/2}$ and a coarse-grained phase-space density $f \sim E^{-5/6}$.

(vii) Once the phase-space spiral has ceased to be re-solved, or its width is no longer negligible, a core is estab-lished and two-body relaxation causes the halo to heat the core.

3 RELEVANCE FOR COSMOLOGY

Has the toy model any relevance for realistic three-dimensional systems? The interplay between phase mixing and violent relaxation that it so clearly illustrates is cer-tainly generic and as such relevant to nearly spherical sys-tems. The period at which a star oscillates radially in a spherical potential is strictly a function of both energy and angular momentum. However, in a typical galactic potential the radial period of a star is largely determined by the star's energy.[2] Consequently, motion in the (r, p_r) phase plane is closely analogous to the motion in the (x, p_x) plane stud-ied in the last section. The shells or ripples that are seen in unsharp-masked images of a significant fraction of ellip-tical galaxies (Malin & Carter 1983) are manifestations of the winding up of an initially narrow distribution of stars in the (r, p_r) phase plane (Hernquist & Quinn 1988) very much like what we see in Fig. 1.

As Zel'dovich (1970) pointed out, the non-linear stage in cosmic structure formation is initially a one-dimensional process. It gives rise to the network of very overdense sheets that are now familiar as the 'filaments' of the 'cosmic web' that are seen in slices cut through computer simulations of gravitational clustering (Shandarin et al., 1995). The forma-tion of such a virgin sheet will closely parallel the dynamics of the last section. Differences of detail will arise early on through the continued transverse expansion of the matter, which makes the force acting between two wafer-thin slices of matter an explicit function of time, but these differences are likely to be unimportant, given the finite duration of the one-dimensional relaxation process, and the tendency of the motion in the perpendicular directions to be faltering and

---

[2] The dependence on L vanishes entirely in the case of the isochrone potential.

turning to contraction soon after a singularity is reached in the first direction.

Thus virgin sheets of the cosmic web will have singular central densities $\rho \sim x^{-1/2}$. The characteristic transverse length scale of these first sheets depends upon the power spectrum of the initial fluctuations. Unless the power spectrum has a sharp cutoff, many different length scales will characterize the transverse structure of the virgin sheets within a sufficiently large volume of space because many different linear modes combine to determine how and when a given part of the Universe will go non-linear and collapse.

Eventually the sheets collapse transversely, either upon themselves or through falling onto the massive objects that tend to form at the nodes of the original cosmic web. During this second stage of structure formation, violent relaxation can occur again. It may be possible to idealize the dynamics as occurring in the phase plane defined by the direction of fastest infall, y, and its conjugate momentum. In this plane an initially narrow distribution of phase points will be wound up into a spiral, and the final density profile is likely to be a cusped function $\rho_y \sim y^{-\beta}$ with $\beta > 0$. The strong initial inhomogeneity of the system will result in the spiral winding up much more rapidly than it does when a virgin sheet forms, so we expect $\beta < \frac{1}{2}$. Finally the over-dense tube resulting from collapse in the x and y directions will collapse along its length, z. Again a cusped final density profile in z is to be expected, $\rho_z \sim z^{-\gamma}$, but violent relaxation will not be efficient, so $\gamma < \frac{1}{2}$. The final density profile $\rho(r)$ can be thought of as the spherically averaged product of the profiles established in each collapse direction. It is easy to show that $\rho \sim r^{-(\alpha+\beta+\gamma)}$, where $\alpha = \frac{1}{2}$. The exponent of r must thus be greater than $\frac{1}{2}$ and is expected to be significantly less that $\frac{3}{2}$. Simulations of cosmic structure formation favour exponents that lie towards the upper half of this expected range (Hayashi et al. 2003).

3.1 Discreteness in cosmic N-body simulations

We have argued that when a sheet of zero thickness in phase space collapses, the final virialized structure should have a singular central density. We have also shown that there is a maximum phase-space density that can be achieved when a finite number of particles is used to sample the phase-space sheet [eq. (9)]. Here we ask what the maximum phase-space density is that can be achieved in the best current N-body simulations of cosmic structure formation, and inside what radius within a DM halo this restriction becomes important.

We have seen that one of two effects can set an upper bound on the phase-space density that occurs in a simulation. One is due to the termination of violent relaxation by discreteness. For the one-dimensional case it is quantified by eq. (9). The other is set by any upper limit on the initial phase-space density of the initial conditions, since Liouville's theorem forbids any increase in the phase-space density.

It is not evident how to extend eq. (9) to the three-dimensional case. This is unfortunate, for its implication that the highest phase-space densities are associated with the most massive objects, is unexpected. It also needs clarification: it does not apply to objects that form through the merger of virialized pieces. Hence, when there is considerable small-scale power, few if any objects to which it applies will have survived to the present epoch. However, the result does explain why Knebe et al. (2002) found that suppression of small-scale power in the input spectrum did not reduce the cuspiness of the final haloes. Also, it suggests that the material that now forms the cores of simulated haloes virialized in narrow ranges of length-scale and redshift: this material was in the largest structures to collapse before substructure could form within them.

In view of the difficulty of generalizing equation (9) to three dimension, we concentrate on ways in which discreteness effects limit the phase-space density achievable prior to virialization. Below we show that the upper limit on f that we derive from these effects predicts convergence radii for DM haloes in simulations that are in reasonable agreement with those determined empirically. This finding suggests that restrictions on f prior to virialization are dominant in practice.

Prior to virialization discreteness limits f in two ways:

(i) With a small number of sampling points, it is not possible accurately to trace a curved phase-space sheet.

(ii) In simulations the gravitational forces are estimated by concentrating mass into lumps. This concentration adds high-frequency noise to the force field. Neighbouring particles sample this noise in largely uncorrelated ways, and thus acquire uncorrelated components of momentum that are discreteness artifacts. These momentum components broaden an initially perfectly thin sheet of phase points.

We estimate these effects in Appendix A. The second effect is estimated in two complementary ways. In every case we estimate the Poincaré invariant Γ over which two or three particles are distributed in one pair of canonically conjugate coordinates. Since there are three such pairs, our estimate of the DF is

$$f \sim \frac{m}{\Gamma^3}, \tag{10}$$

where m is the mass of a simulation particle.

Equations (A5), (A14), and (A19) give three estimates of Γ. The expressions all contain the dimensional factor $H_0(\Delta q)^2$, where H_0 is the Hubble constant and Δq is the comoving separation of particles at early times. This factor is multiplied by a numerical factor that is comparable to unity, but probably a little smaller. Thus below we use the estimate

$$f \sim \frac{\eta m}{[H_0(\Delta q)^2]^3}, \tag{11}$$

where η is a factor a little smaller than unity. Equation (A4) and equation (A16) independently imply that $f \sim a^{-9/2}$ in the run up to virialization.

When the system virializes, we have argued that the peak phase-space density will decrease only if the phase-space sheet is thinly sampled compared to its width. In Appendix B we show that on virialization the peak value of the DF does not diminish much below that given by equation (11).

4 APPLICATION TO SIMULATIONS

Hayashi et al. (2003) studied the convergence of the central structure of DM haloes in state-of-the art simulations of

structure formation. It is interesting to compare the convergence radius r_{conv} that they derived empirically from these simulations with the one that follows our considerations.

Let us assume that DM haloes have cores in which $\rho(r) = \rho_0(r/r_0)^{-1}$ and the velocity dispersion tensor is isotropic – simulations suggest that these assumptions are not seriously violated. Then, with the gravitational potential taken to be zero at the centre, the distribution function of the system is easily shown to be

$$f(E) = \frac{3G\rho_0^2 r_0^2}{(2E)^{5/2}}. \tag{12}$$

We find the radius $r_{\min}$ at which the DF from this formula at $v = 0$ equals the maximum phase density of equation (11). We find

$$r_{\min}^{5/2} = \frac{3[H_0(\Delta q)^2]^3}{32\pi^{5/2}G^{3/2}(\rho_0 r_0)^{1/2}\eta m}. \tag{13}$$

As one proceeds inwards from $r_{\min}$, more and more of the density is contributed by parts of phase space at which the DF exceeds the value of eq. (11). In a simulation these portions of phase space are under-populated, so the density falls more and more below its true power-law value. Hence $r_{\min}$ is our prediction of the convergence radius of a simulated halo.

If N^3 particles are used to represent the matter in a box of side L, the mass of an individual particle is

$$m = \Omega_{\mathrm{m}}\frac{3H_0^2}{8\pi G}\left(\frac{L}{N}\right)^3, \tag{14}$$

and $r_{\min}$ satisfies

$$r_{\min}^{5/2} = \frac{H_0 L^3}{4\pi^{3/2}(G\rho_0 r_0)^{1/2}N^3\eta\Omega_{\mathrm{m}}}. \tag{15}$$

We apply this formula to the G1 sequence of models listed in Table 1 of Hayashi et al. For the relevant halo $\rho_0 r_0 = 6.34 \times 10^7 h^{-1}\,\mathrm{M}_\odot(h^{-1}\,\mathrm{kpc})^{-2}$, while $L = 5h^{-1}\,\mathrm{Mpc}$, so

$$r_{\min} = 2.14(\eta\Omega_{\mathrm{m}}/0.3)^{-2/5}(N/256)^{-6/5}h^{-1}\,\mathrm{kpc}. \tag{16}$$

As one proceeds from $N = 32$ to $N = 256$ down the G1 sequence of models, we find that $\eta^{2/5}r_{\min}/r_{\mathrm{conv}} = 1.14$, 1.47, 1.53, and 1.53. So $r_{\min}$ is larger than r_{conv} by a factor $\sim 1.5\eta^{-2/5}$ that is only slightly greater than unity. This agreement between our analytic estimates and the numerical studies suggests that the peak densities within simulated haloes are indeed set by discreteness effects that operate before virialization.

5 CONCLUSIONS

Semi-analytic work on the formation of cosmic structure usually focuses on the collapse of spherical overdensities (Gunn & Gott 1972; Fillmore & Goldreich 1984; Bertschinger 1985; Subramanian, Cen & Ostriker, 2000). Actually one direction collapses before the other two, so the crucial first phase of the virialization process is one-dimensional (Zel'dovich, 1970; Shandarin et al., 1995). Fillmore & Goldreich (1984) obtained a self-similar solution of the collapse problem in this planar symmetry. Unfortunately, their results are not directly comparable to ours because (i) they assumed that the transverse expansion continued unperturbed, and (ii) their initial overdensity was

constrained to diverge at the centre of the sheet. Consequently, for all $t > 0$ their solution has a collapsed core, and the phase-space spiral has a time-invariant form: its scale changes with time, but it does not wind up in the manner of Fig. 1.

Our toy model of the planar collapse of CDM reveals a strong interplay between phase mixing and violent relaxation, in which an initially small phase lag of the oscillations between the centre and periphery of an overdensity causes energy to flow outwards, and this outward energy flow hastens the growth of the phase difference, which in turn causes the exchange of energy to repeat on ever smaller scales. The numerical evidence suggests that in the limit of arbitrarily many particles, power-law profiles in space and energy would be established as a natural consequence of the large dynamic range between the smallest scale of energy interchange and the overall size of the system. Power laws are also consistent with the original infinite phase-space density persisting at the centre of the relaxed system, while admixture of 'air' ensures that the phase-space density is finite and outwards-decreasing elsewhere.

When the system is represented by only a finite number of particles, random motions develop prior to virialization. Consequently, as collapse begins, the phase-space density is finite and the interplay between phase mixing and violent relaxation is prematurely terminated. The central phase-space density of the relaxed system is comparable to the phase-space density just before collapse, while further out it differs little from the value that would hold in the limit of an arbitrary number of particles. Consequently, the real-space density profile must turn over near the centre from the slope it would have in that limit.

An interesting result from the one-dimensional model is that, in a given simulation, the peak phase-space density in simulated sheets of the cosmic web scales with particle number as $f \sim n^{3/2}$. Hence, the sheets with the highest surface density achieve the largest phase-space density. The surface density of the sheets that form is increased if we suppress small-scale power in the initial fluctuation spectrum, so there is a suggestion that simulations that have little small-scale power will produce the cuspiest haloes. This finding is consistent with the counter-intuitive results of Knebe et al. (2002).

The extension to the formation of DM haloes of these results for the formation of the sheets of the cosmic web is not straightforward. Some insight can be gained by imagining that the original process repeats as each of the other directions experiences collapse. This idealization is problematic because the collapses of these directions are rarely well separated in time. However, it is probably legitimate to argue that in the limit of infinite particle number, the final density profile should be a power law[3] because the collapsing sheet brings no relevant scale into the relaxation process, and the latter has no intrinsic scale. Also it seems likely that violent relaxation will be less efficient in later collapses than it was in the first, because the phase spirals associated with these directions will wind up very quickly. This reasoning

---

[3] Figure 4 of Hayashi et al. (2003) argues against this conclusion, however.

allows us to set an upper limit $\frac{3}{2}$ on the power-law index of the final density cusp, which is clearly greater than $\frac{1}{2}$.

If we assume that in the limit of infinite particle number the slope would be $\alpha = 1$, as in the NFW profile, then we can estimate the radius $r_{\min}$ at which the maximum phase-space density sampled equals the phase-space density that developed prior to virialization. This radius forms a reasonable estimate of the radius at which the simulated density profile turns away from a line of unit slope. We find that $r_{\min}$ is larger by a factor ~ 2 than the convergence radius r_{conv} of Hayashi et al. (2003). This finding strongly suggests that processes that take place prior to virialization determine the smallest radius at which a simulated halo can be trusted.

The importance of knowing which structures in cosmological simulations are reliable, is clearly very great. Brute-force convergence studies such as those of Power et al. (2003) do not constitute a straightforward tool for validating N-body simulations because the limit in which reality is approached involves sending three quantities to zero: the mass of an individual particle, the softening length, and the wave-length of the highest-frequency mode included in the initial conditions. Before an entirely convincing convergence study can be made, one needs to know along which path in the three-dimensional space of these parameters one should approach the origin (e.g., Splinter et al. 1998). Hitherto there has been a tendendcy for N-body simulators to focus on the impact that discreteness has on the dynamics of relaxed systems. This study suggests that dicreteness may have its dominant impact prior to virialization.

AKNOWLEDGMENTS

REFERENCES

Bertschinger E., 1985, ApJS, 58, 39
Binney J., Knebe A., 2002, MNRAS, 333, 378
Fillmore J.A., Goldreich P., 1984, ApJ, 281, 1
Fukushige T., Kawai A., Makino J., 2003, astro-ph/0306203
Gunn J.E., Gott J.R., 1972, ApJ, 176, 1
Hayashi E., Navarro J.F., Power C., Jenkins A., Frenk C.S., White S.D.M., Springel V., Stadel J., Quinn T., 2003, astro-ph/0310576
Hernquist L., Quinn P.J., 1988, ApJ, 331, 682
Jing Y.P., Mo H.J., Borner G., Fang L.Z., 1995, MNRAS, 276, 411
Klypin A., Kravtsov A.V., Bullock J.S., Primack J.R., 2001, ApJ, 554, 903
Knebe A., Devriendt J.E.G., Mahmood A., Silk J., 2002, MNRAS, 329, 813
Kuhlman B., Melott A.L., Shandarin S.F., 1996, ApJ, 470, L41
Lynden-Bell D., 1967, MNRAS, 136, 101
Malin D.F., Carter D., 1983, ApJ, 274, 534
Melott A.L., 1983, ApJ, 264, 59
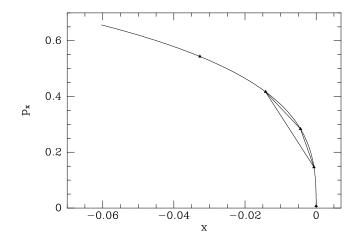Melott A.L., Shandarin S.F., Splinter R.J., Yasushi S., 1997, ApJ, 479, 79

Figure A1. An underlying Zel'dovich wave.

Navarro J.F., 2003, in IAU Symposium 208, *astrophysical Super-Computing Using Particles*, ed. J. Makino & P. Hut
Power C., Navarro J., Jenkins A., Frenk C.S., White S.D.M., Springel V., Stadel J., Quinn T., 2003, MNRAS, 338, 14
Shandarin S.F., Melott A.L., McDavitt K., Pauls J.L., Tinker J., 1995, PhRvL, 75, 7
Splinter R.J., Melott A.L., Shandarin S.F., Suto Y., 1998, ApJ, 497, 38
Subramanian K., Cen R., Ostriker J.P., 2000, ApJ, 538, 528
Taylor J.E., Navarro J.F., 2001, ApJ, 563, 483
White S.D.M., 1996, *Cosmology and Large-Scale Structure, Les Houches Session LX*, eds. Schaeffer R., Silk J., Spiro M., Zinn-Justin J., Elsevier 1996, p. 349
Zel'dovich, Ya.B., 1970, A&A, 5, 84

APPENDIX A: WIDTH OF PHASE SHEET

The initial conditions for cosmological simulations are invariably set up by superposing a number of plane-wave perturbations to the density and velocity fields. Comoving coordinates are generally employed rather than the inertial coordinates employed in Section 2. In canonically conjugate comoving coordinates, Zel'dovich's (1970) analytic solution for the evolution of an isolated wave is

$$x = q + F$$
$$p = a^2 H F, \tag{A1}$$

where $H = \dot{a}/a$ is the Hubble constant at scale factor a and we adopt

$$F = -\frac{a}{a_0 k} \sin(kq). \tag{A2}$$

Here q is a Lagrangian coordinate and a_0 is the scale factor at which the wave breaks and a caustic forms.

A1   Effective width of a distorted sheet

The phase-space density of a group of particles is calculated by evaluating the phase-space volume that they occupy. By definition, the latter is the product of three Poincare invariants $\Gamma_i = \int \mathrm{d}x_i \mathrm{d}p_i$, one for each index i, with p_i the momentum conjugate to x_i. Consider therefore Fig. A1, which shows the track in the (x_1, p_1) plane of a collapsing wave, and a number of particles that are intended to realize this

wave in a simulation. Any three consecutive particles define a triangle. We now evaluate the area of this triangle, which is the Poincaré invariant that the particles define.

Taking the modulus of the vector product $(x_1 - x_2, p_1 - p_2) \times (x_2 - x_3, p_2 - p_3)$ of two differences between three vectors (x, p) of the form (A1), we find the Poincaré invariant

$$\Gamma = \frac{Ha^2}{2} [(q_1 - q_2)(F_2 - F_3) - (q_2 - q_3)(F_1 - F_2)] \qquad (A3)$$

If we now expand F_1 and F_3 as Taylor series around q_2, we find to leading order

$$\Gamma = \frac{1}{4} Ha^2 F''(q_2)(q_2 - q_1)(q_3 - q_2)(q_3 - q_1)$$
$$= \frac{Ha^3 k}{2a_0} \sin(kq)(\Delta q)^3, \qquad (A4)$$

where in the last line we have assumed that the particles are uniformly spaced in q with interparticle separation Δq. In a flat universe, $H = a^{-3/2} H_0$, where H_0 is the Hubble constant at the current epoch, and we see from equation (A4) that $\Gamma \sim a^{3/2}$. This estimate of Γ is credible up to the epoch of virialization, $a = a_0$. Hence, at virialization the particles occupy a minimum Poincaré invariant

$$\Gamma = H_0(\Delta q)^2 \left[\frac{1}{2}(k\Delta q)a_0^{1/2} \sin(kq)\right]. \qquad (A5)$$

This expression for the Poincaré invariant is made up of a dimensional factor

$$\Gamma_0 = H_0(\Delta q)^2, \qquad (A6)$$

and a dimensionless factor

$$\eta = \frac{1}{2}(k\Delta q)a_0^{1/2} \sin(kq)$$
$$\simeq \frac{1}{2}(k\Delta q)^2 a_0^{1/2} \qquad (A7)$$

where the second line follows because a wave breaks, and a high-density virialized structure forms, around $q = 0$. At the Nyquist frequency, $k\Delta q = \pi$, so this factor will be of order, but less than unity is cases of interest. The other two factors are each $\sim \frac{1}{2}$. Hence, equation (A6) gives a useful order-of-magnitude estimate of the smallest achievable value of Γ.

A2 Unequilibriated fluctuations

The process of setting up a cosmological simulation can be conceptualized as a two-stage process. One first sets up a discrete representation of a perfectly homogeneous distribution of matter, and then one perturbs it by displacing particles in a systematic way that generally involves waves of some kind. Let us focus on potential fluctuations implicit in the unperturbed 'homogeneous' distribution of particles, since these fluctuations are clearly an artifact due to discreteness. The nature of these fluctuations is elucidated by the 'glass' approach to realizing a homogeneous matter distribution. In this technique (White, 1996) particles are first distributed randomly within the simulation volume and are then moved subject to the usual equations of motion with gravity made into a repulsive force. After a sufficient number of integration steps, each particle comes to rest at the bottom of its nearest potential well. When gravity is restored to an attractive force, the potential well becomes a hill with the particle at its summit. When particles are distributed on a lattice, they again arrive at the summits of hills, and the structure of these hills can be investigated by Ewald summation.

When the 'homogeneous' configuration is perturbed, the hills are distorted, but only mildly if, as should be the case, the perturbation is imposed at sufficiently large redshift for the imposed displacements to be small compared to the inter-particle separation. Since the structure of an individual hill depends on the positions of *all* particles, each particle is displaced slightly from the summit of its own hill, and will roll down the hill as soon as the simulation is integrated forward in time. Its rolling motion is nothing but a discreteness artifact and will cause the Poincaré invariant associated with neighbouring particles to grow as $p_r \Delta q$, where p_r is the momentum of a typical particle's roll.

Let the parabolic form of the potential around the summit be

$$\Phi(x) = -\frac{\Phi_0}{2(\Delta q)^2} x^2, \qquad (A8)$$

where Φ_0 is an appropriate constant. Then from the Hamiltonian $\frac{1}{2}p^2/a^2 + \Phi/a$ we easily find that x satisfies the equation of motion

$$x'' + \frac{3}{2}\frac{x'}{a} - \frac{\Phi_0}{(H_0\Delta q)^2}\frac{x}{a^2} = 0, \qquad (A9)$$

where a prime denote differentiation with respect to a and an Einstein-de Sitter cosmology has again been assumed. This homogeneous equation has solutions $x \propto a^n$, where

$$n = -\frac{1}{4}\left(1 \pm \sqrt{\frac{16\Phi_0}{(H_0\Delta q)^2} + 1}\right). \qquad (A10)$$

On dimensional grounds $\Phi_0/(H_0\Delta q)^2 \sim 1$, so the value of n for the growing solution is

$$n_g = \frac{\Phi_0^{1/2}}{H_0\Delta q} - \frac{1}{4} + \frac{H_0\Delta q}{32\Phi_0^{1/2}} + \cdots$$
$$\simeq \frac{\Phi_0^{1/2}}{H_0\Delta q} - \frac{1}{4}. \qquad (A11)$$

Inserting $x = x_0(a/a_0)^{n_g}$, where x_0 and a_0 are constants to be determined, into $p_r = a^{3/2}H_0 x'$, we find that the Poincaré invariant associated with neighbouring particles is

$$\Gamma = x_0 \Phi_0^{1/2}(a/a_0)^{n_g + 1/2}. \qquad (A12)$$

By Ewald summation we find that the potential (A8) governing the displacement of a single particle from its position in the lattice has coefficient

$$\Phi_0 = \frac{3}{2\pi}(H_0\Delta q)^2. \qquad (A13)$$

With this value of Φ_0 equations (A11) and (A12) yield

$$\Gamma = \sqrt{\frac{3}{2\pi}}(a/a_0)^{0.94}(H_0\Delta q x_0). \qquad (A14)$$

If we set a_0 equal to the expansion factor at which virialization occurs, then x_0 becomes the magnitude of the particle's displacement at this epoch, and will therefore be a significant fraction of Δq. Consequently, our new estimate of Γ is similar to that of equation (A5).

A3 Graininess of the Potential

Since the gravitational force is calculated from the positions of a finite number of particles rather than the density field

of the true continuum, it contains spurious high-frequency structure. A lower limit on the magnitude of this structure is given by the force from the nearest neighbour – in a collisionless system, forces from neighbours should always be small compared to the overall force. The contribution that this makes to the spurious velocity of a particle is

$$\delta v = \int dt\, \frac{Gm\Delta x}{a^2[(\Delta x)^2 + \epsilon^2]^{3/2}}, \tag{A15}$$

where we have assumed that Plummer softening is being used and v is the true peculiar velocity. Substituting for Δx from equation (A1), and again assuming a flat cosmology, this becomes

$$\delta v = \frac{Gm}{H_0(\Delta q)^2}$$
$$\times \int_0^{a_0} \frac{da\,[1 - (a/a_0)\cos(k\Delta q)]}{a^{1/2}\{[1 - (a/a_0)\cos(k\Delta q)]^2 + (\epsilon/\Delta q)^2\}^{3/2}} \tag{A16}$$

The expression in braces on the bottom of the integrand starts near unity and tends to $(\epsilon/\Delta q)^2$. Typically the softening length ϵ is a significant fraction of Δq, so the total variation of this term is not large. The square bracket on the top starts at unity and vanishes abruptly when $a \simeq a_0$. Hence, the dominant variation of the integrand comes from the factor $a^{1/2}$ on the bottom, and a reasonable approximation is

$$\delta v = \frac{2Gma_0^{1/2}}{H_0(\Delta q)^2}. \tag{A17}$$

Multiplying by $a_0\Delta x$ we obtain an estimate of the Poincaré invariant generated by graininess of the potential

$$\Gamma = (\delta v)(a_0\Delta x) = \frac{2Gm}{H_0\Delta q}a_0^{3/2}[1 - (a/a_0)\cos(k\Delta q)]. \tag{A18}$$

In a flat, matter-dominated cosmology, $Gm/\Delta q = (H_0\Delta q)^2/16$, so this equation can be written

$$\Gamma = H_0(\Delta q)^2\frac{a_0^{3/2}}{8}[1 - (a/a_0)\cos(k\Delta q)], \tag{A19}$$

which is very again similar to equation (A5).

APPENDIX B: EFFECT OF VIRIALIZATION

Fig. B1 shows a phase-space distribution of points that is rather sparsely sampling a Zel'dovich wave as it collapses. From this point on the coarse-grained phase-space density will at most points decline rapidly as the sheet wraps round and round itself, trapping ever more air in the roll. So let us ask what the smallest Poincaré invariant is that we could associate with the n particles nearest the centre of the roll. We take this to be the shaded rectangle. Its invariant is

$$\Gamma_n = \left(n\Delta q - \frac{\sin(nk\Delta q)}{k}\right)H_0a_0^{1/2}\frac{\sin(nk\Delta q)}{k}$$
$$\simeq H_0(\Delta q)^2\left[\frac{n^4}{3!}a_0^{1/2}(k\Delta q)^2\right]. \tag{B1}$$

Again the dimensional factor $H_0(\Delta q)^2$ emerges, but this time multiplied by a numerical factor that is larger by $n^4/3$ than the corresponding one in equation (A5). This factor is not large for a sparsely sampled wave, and violent relaxation
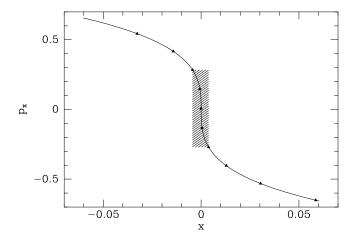

Figure B1. Shaded region shows estimate of the Poincareé invariant occupied by the central 5 points after virialization.

makes the estimate inapplicable to the case of a densely sampled wave. We conclude that on virialization the peak phase-space density does not decline strongly.